Journal of
Materials Chemistry B

Accepted Manuscript

This article can be cited before page numbers have been issued, to do this please use: M. Zhang, H. Han, S. Zhang, C. Wang, Y. Lu and W. Zhu, *J. Mater. Chem. B*, 2017, DOI: 10.1039/C7TB02323E.

ROYAL SOCIETY OF CHEMISTRY

rsc.li/materials-b

DOI: 10.1039/C7TB02323E

Journal Name

ARTICLE

A new colorimetric and fluorescent probe with a large stokes shift for rapid and specific detection of biothiols and its application in living cells

Received 00th January 20xx,
Accepted 00th January 20xx

DOI: 10.1039/x0xx00000x

www.rsc.org/

Meng-Zhao Zhang[a], Hai-Hao Han[a], Shao-Ze Zhang[b], Cheng-Yun Wang[a,*], Yun-Xiang Lu[b] and Wei-Hong Zhu[a,*]

In this work, a new reversible colorimetric and fluorescent probe for sequential recognition of copper ions and biothiols is synthesized easily. Based on the chelation–enhanced fluorescence quenching (CHEQ) effect, this probe shows high sensitivity and selectivity towards Cu^{2+}, which can be detected by naked eyes. And this experimental phenomenon can be recovered upon addition of biothiols, restoring its initial fluorescence intensity. This probe also features a very high response speed (less than 5 seconds) and a large stokes shift (178 nm) toward Cu^{2+} and biothiols. Moreover, the detection limit for Cu^{2+} and biothiols are as low as 7.34 nM and 10.3 nM, respec8vely. Addi8onally, this ON−OFF−ON–type fluorescence recognition circle can be repeated more than 5 times by addition of Cu^{2+} and biothiols in turn. Particularly, this 1−Cu^{2+} ensemble is further successfully applied for GSH detection in living cells.

Introduction

Biological thiols, such as glutathione (GSH), cysteine (Cys) and homocysteine (Hcy), play critical roles in physiological and pathological processes.[1-5] While abnormal levels of these biothiols have been shown to be associated with various human diseases.[6] For example, elevated Cys is known to be associated with many syndromes such as retarded growth, hair depigmentation edema, lethargy and liver damage[7]; elevated Hcy might cause Alzheimer's, cardiovascular diseases, neural tube effect, inflammatory bowel disease, and osteoporosis.[8] Specifically, GSH is the most abundant cellular thiol, it plays an essential role in maintaining biological redox homeostasis.[9,10] In light of the aforementioned examples, efficient monitoring of biothiols in live cells is crucial for identifying abnormal biological processes and risk towards diseases.[11] Therefore, an efficient method for selective discrimination of biothiols in biological systems is urgently required for better physiological and pathological analysis and early diagnostics.[12]

Some methods have been attempted to discriminate biothiols, such as high–performance liquid chromatography (HPLC)[13], UV–vis absorption spectrophotometry[14], capillary electrophoresis[15], potentiometry[16], mass spectrometry (MS)[17] and fluorescent technique[18–21]. Among these various analytical methods that are available, fluorescent probes possess innate advantages owing to its sensitivity, selectivity, simplicity and real-time detection.[22-26] To date, a number of fluorescent probes have been developed for distinguishing biothiols from other amino acids. These probes are mainly based on five types of reactions: (1) cleavage of sulfonamide/sulfonate ester by biothiols[27,28]; (2) Michael addition[29,30]; (3) cyclization with aldehyde[31,32]; (4) cleavage of disulfide by thiols[33-35]; (5) intramolecular elimination[36,37]. To best of our knowledge, most organic reaction based fluorescent probes suffered two main shortages: required strictly conditions and time–consuming, thus limited the application of these probes.[38]

Due to its excellent features in donor-π-acceptor (D-π-A) structure, near infrared emission wavelength and large Stokes shift[39,40], dicyanoisophorone based dyes are well known in Dye-sensitized solar cells[41,42] and organic nonlinear optical crystals[43-45]. Our group had long-standing exploration for the synthesis and application of this kind of fluorescence materials.[23] In this work, we synthesized a new biothiols fluorescence probe (Compound 1) based on dicyanoisophorone fluorescent dye (Scheme 1). As expected, Compound 1 could coordinated with Cu^{2+} through hydroxyl group to form 1–Cu^{2+} and the subsequent complex 1–Cu^{2+} could be developed as a platform for biothiols real–time detection. This probe exhibited excellent sensing properties, high sensitivity and selectivity for biothiols with remarkable fluorescence enhancement and a large Stokes shift ($\lambda_{em} - \lambda_{abs}$ = 178 nm). Additionally, the potential utility of this ON−OFF−ON and colorimetric fluorescence probe was successfully used to detect biothiols in living cells.

Experimental

Synthesis of Compound 2

3,5,5-Trimethyl-2-cyclohexen-1-one (3.0 g, 21.7 mmol), malononitrile (1.72 g, 26.0 mmol) and piperidine (0.3 g, 2.9 mmol) were dissolved in absolute EtOH (50.0 mL). The mixture was heated

[a] Key Laboratory for Advanced Materials and Institute of Fine Chemicals, School of Chenmistry and Malecular Engineering, East China University of Science and Technology, 130 Meilong Road, Shanghai 200237, PR China. E-mail: cywang@ecust.edu.cn (C-Y Wang); whzhu@ecust.edu.cn (W-H Zhu).
[b] Department of Chemistry, School of Chemistry and Molecular Engineering, East China University of Science & Technology, 130 Meilong Road, Shanghai 200237, P. R. China.
Electronic Supplementary Information (ESI) available: [details of any supplementary information available should be included here]. See DOI: 10.1039/x0xx00000x

View Article Online
DOI: 10.1039/C7TB02323E

at 90 °C for 13 h under N_2 atmosphere. After the mixture was cooled and the solvent was removed, then the residue was dissolved in CH_2Cl_2, washed with water, and dried over Na_2SO_4. Finally, the solvent was concentrated by rotary evaporation to obtain the raw product, which was purified by silica chromatography (Petroleum/Ethyl acetate = 3/1) (2.88 g, 61%, Mp: 73-75 °C). ^{1}H–NMR (400 MHz, $CDCl_3$): δ = 6.62(s, 1H), 2.52 (s, 2H), 2.18 (s, 2H), 2.03 (s, 3H), 1.00 (s, 6H) (Fig. S1). ^{13}C–NMR (100 MHz, $CDCl_3$): δ = 170.24, 156.72, 147.93, 145.56, 138.74, 127.64, 126.16, 121.25, 120.95, 115.80, 114.71, 114.17, 113.31, 74.54, 42.30, 38.16, 31.63, 27.41. (Fig. S2).

Synthesis of Compound 1

Compound 2 (500 mg, 2.7 mmol), 3,4–dihydroxybenzaldehyde (320 mg, 2.7 mmol) and five drops of piperidine were dissolved in 30 mL of acetonitrile. The mixture was heated to reflux for 9 h under N_2 atmosphere, and the solvent was removed by rotary evaporation. The resulting residue was dissolved in dichloromethane, then washed with water and dried over anhydrous $MgSO_4$. The crude product was purified by silica chromatography (eluted with Petroleum/Ethyl acetate = 5/2, v/v) to afford an orange solid (610 mg, 77% yield, Mp: 186-188 °C). ^{1}H NMR (400 MHz, DMSO–d_6): δ = 9.61 (s, 1H), 9.08 (s, 1H), 7.13 (m, 3H), 7.03 (d, J =8 Hz, 1H), 6.80 (s, 1H), 6.75 (d, J= 8 Hz, 2H), 2.60 (s, 2H), 2.52 (s, 2H), 1.01 (s, 6H). (Fig. S3) ^{13}C NMR (100 MHz, d_6–DMSO, Me_4Si) δ (ppm) 170.24, 156.32, 147.92, 145.57, 138.74, 127.65, 126.17, 121.26, 120.95, 115.81, 114.71, 114.17, 113.31, 74.55, 42.31, 38.17, 31.63, 21.42. (Fig. S4) ESI–MS: calculated $[C_{19}H_{18}N_{52}O_2 – H]^+$ 305.1290; found 305.1287 (Fig. S5).

Characterization

All chemical reagents and solvents were analytical grade and purchased from commercial suppliers. ^{1}H NMR and ^{13}C NMR spectra were collect in $CDCl_3$ and DMSO–d_6 on Bruker AM400 NMR spectrometer. HRMS spectra analyses were carried out with Waters LCT Premier XE spectrometer. Absorption spectra was recorded on a Varian Cary 500 spectrophotometer, and fluorescence spectra was performed on F97pro fluorospectrophotometer.

DFT calculations

At the method level of B3LYP/cc–Pvdz, the geometries of the isolated molecule and coordination complex were fully optimized.[47,48] No symmetry or geometry constraint was imposed during the optimizations. Frequency calculations were implemented at the same theoretical levels to corroborate that all the structures were genuine minima on the potential energy surface. Then, the molecular orbital analyses were performed by Multiwfn program.[49,50] The color–filled isosurfaces of highest occupied molecular orbitals (HOMOs) and lowest unoccupied molecular orbitals (LUMOs) were visualized by means of the VMD package.

Cell culture

HepG2 was incubated in a Dulbecco's Modified Eagle's Medium (Invitrogen, Carlsbad, CA, USA) supplemented with 10% fetal bovine serum (Gibco, Gland Island, NY, USA). The HepG2 cells were cultured according to previously report.[51] Briefly, the cells were incubated with Compound 1 for 15 min, then incubated with Cu^{2+} for 30 min, finally incubated GSH for 30 min. After that, the cells were stained with Hoechst 33342 (5 μg mL^{-1}) at 37 °C for 5 min. Then, cells were washed with PBS (phosphate buffered saline) three times, recorded using an Operetta high content imaging system (Perkinelmer, US) at an excitation wavelength of 460–490 nm and an emission wavelength of 560–630 nm, quantified and plotted by columbus analysis system (Perkinelmer, US).

Cell viability assay

The HepG2 cells were cultured according to previously report.[48] Briefly, the cells were plated on 96–well plates at 8000 cells per well in growth medium. The cells were incubating for 24 h upon addition of 100 μL of serum–free DMEM to 10 μL per well of MTS/PMS (20:1, Promega Corp) solution. After incubation at 37 °C under 5% CO_2 for 2-4 h, the absorbance was recorded at 490 nm by M5 microplate reader (Molecular Device, USA).

Result and discussion

Synthesis route

This probe was easily synthesized with high yields in two steps (Scheme 1), the detailed characterization dates were presented in the Supporting information.

Absorption and emission properties about Compound 1 and Cu^{2+}

Fig. 1 showed the absorbance and fluorescence spectra of Compound 1 upon addition of Cu^{2+} in HEPES bu□er solution (containing 10% DMSO, pH = 7.4, 50 mM). Compound 1 showed intense absorption band centered around 429 nm (ε = 2.3 × 10^4 M^{-1} cm^{-1}, Φ^a = 0.062, Table S2) and strong emission peak centered around 607 nm (Fig. 1A and 1B). After addition of Cu^{2+} (20 μM) lead to a decrease in absorption band at 429 nm, at the same time, a new growth of absorbance band at 505 nm formed (ε = 1.6 × 10^4 $M^{-1}cm^{-1}$, Φ^a = 0.012, $\Delta\lambda_{abs}$ = 76 nm, Table S2). Additionally, a considerable color change from yellow to pink was obvious to be detected by the naked eyes. This could be explained by the stabilization of charge in the excited state after the formation of 1–Cu^{2+} complex which enhanced the ICT mechanism and gave a red shift.[42] At the same time, the fluorescence emission band at 607 nm decreased sharply (Fig. 1B). What's more, both absorbance and fluorescence spectra kept stable within 5 s, which was much faster than most of the previous reports (Fig. S6, Table S1).

To further evaluate the Cu^{2+}–responsive sensitivity of Compound 1, the fluorescence titration experiments in HEPES bu□er solution (containing 10% DMSO, pH = 7.4, 50 mM) was investigated. The absorbance ratio A_{505}/A_{429} before adding Cu^{2+} was 0.13, however it was increased to 2.06 when the concentration of Cu^{2+} was 20 μM (Fig. 2). And the fluorescence intensity at 607 nm before adding Cu^{2+} was 737.26, but it was decreased to 69.69 when the concentration of Cu^{2+} was 20 μM (quenching e□ciency $(I_0 – I)/I_0$ × 100% = 90.6%). The corresponding signal to background ratio of absorbance and fluorescence spectra were calculated to be 15.85 and 32.68,

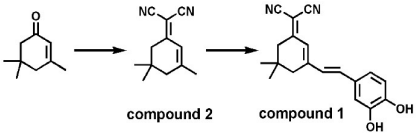

Scheme 1. Synthetic route of Compound 1

View Article Online
DOI: 10.1039/C7TB02323E

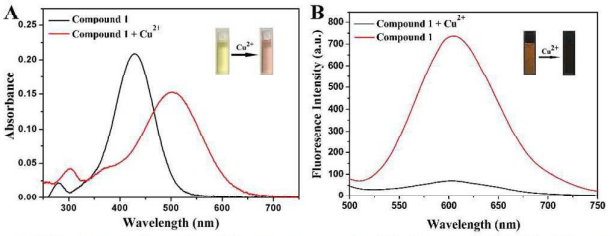

Fig. 1. UV–vis absorption (A) and fluorescence spectra (B) of Compound 1 (10 μM) upon addition of Cu^{2+} (20 μM). All spectra were recorded in DMSO/HEPES buffer solution (10/90, v/v, pH = 7.4, 50 mM). λ_{ex} = 429 nm. Inset (A): Color change of Compound 1 in DMSO/HEPES buffer solution after addition of Cu^{2+} (20 μM). Inset (B): fluorescence change of Compound 1 in DMSO/HEPES buffer solution after addition of Cu^{2+} (20 μM).

respectively (Fig. 2B, Fig. 2D), revealing that Compound 1 was considerable sensitive to Cu^{2+}. What's more, Fig. 2D showed a good linearity (R=0.9963) with respect to Cu^{2+} over concentration range (0–8 μM) and a detection limit of 7.34 nM at 3 σ/κ. Additionally, 1:1 bonding mode was found in the Job plot (Figure S7, Supporting Information) between Compound 1 and Cu^{2+} ions (Scheme 2). Additionally, the binding constant (K) was demonstrated to be 1.61×10^5 (Fig. S8) using Benesi–Hildebrand plot.[32] As shown in the IR spectrum of Compound 1 and 1-Cu^{2+} (Fig. S9A), the peaks (3298.8 and 1336.9 cm^{-1}) of Compound 1 were assigned to vibrational bands of O-H group. Upon addition of Cu^{2+}, a peak at 3298 cm^{-1} was disappeared (Fig. S9B). Moreover, a peak at 621.3 cm^{-1} formed, which assigned to vibrational bands of Cu-O group. Additionally, 1-Cu^{2+} was confirmed by HRMS (Fig. S10), where a dominant peak at m/z value of 368.0377 (calcd 368.0568) corresponds to $[1\text{-}Cu^{2+} + H]^+$. On the basis of the above experiment results, 1:1 bonding mode was confirmed between Compound 1 and Cu^{2+}.

To our delight, the addition of K^+, Na^+, Ni^+, Ag^+, Mg^{2+}, Mn^{2+}, Ba^{2+}, Zn^{2+}, Ca^{2+}, Cd^{2+}, Hg^{2+} and Fe^{3+} (100 μM) had no spectral or visual change on fluorescence emission and absorbance spectra (Fig. S11, Fig. S12). While upon addition of 2 equiv Cu^{2+}, the fluorescence intensity at 607 nm quenched sharply (quenching efficiency 90.6%), indicating that Compound 1 featured an excellent property to Cu^{2+} because of the chelation–enhanced fluorescence quenching (CHEQ) effect.[46] Moreover, a non-negligible change in

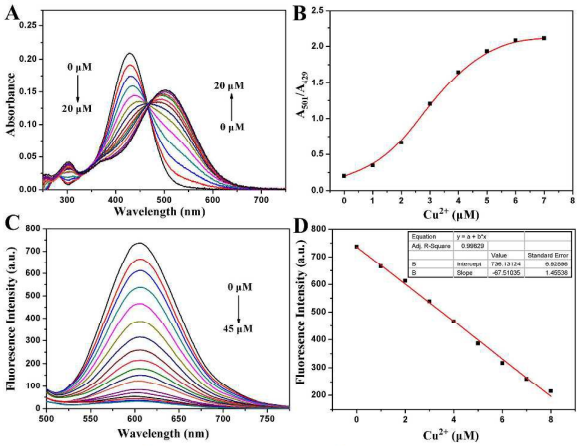

Fig. 2. UV–vis (A) and Fluorescence spectra (C) of Compound 1 (10 μM) towards different concentrations of Cu^{2+} (0–45 μM) in DMSO/HEPES buffer solution (10/90, v/v, pH = 7.4, 50 mM). Plots of (B) absorbance ratio A501/A429 and (D) fluorescence intensity ratio vs. Cu^{2+} concentration (0–8 μM). λex = 429nm.

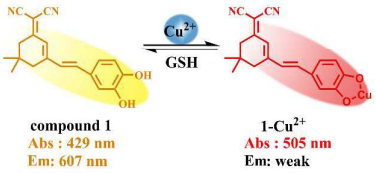

Scheme 2. Proposed sensing mechanism of Compound 1 and 1–Cu^{2+} toward Cu^{2+} and biothiols respectively.

emission spectra was observed with Al^{3+} and Pb^{2+} and the decrease in emission intensity was found in order: Cu^{2+} > Al^{3+} > Pb^{2+}. The differences between the quenching effects were so obvious that the Cu^{2+} was easy to be distinguished. The selectivity studies showed good selective ability on the emission intensity in the presence of different competitive common metal ions.

It was prone to deprotonation at neutral pH for the two adjacent –OH group of Compound 1. Additionally, this deprotonation enhanced in the presence of metal ions due to chelation enhanced fluorescence (CHEF) mechanisms, which stabilized the excited state and showed a red shift in the UV–vis spectra.[49] Fig. S13 showed Compound 1 was stable in the pH range from 3 to 7. However, the fluorescence intensity at 607 nm showed a considerable decrease over the pH range from 7 to 10. Due to the deprotonation of two adjacent –OH group of Compound 1, the emission intensity showed considerable decrease at higher pH. Additionally, the fluorescence of Compound 1 couldn't be quenched over the pH range from 3 to 6 in presence of Cu^{2+} (10 μM), which might be ascribed to the protonation of Compound 1 in acid conditions, which blocked coordination process. Therefore, Compound 1 can be used as a reliable fluorescence probe for detecting Cu^{2+} in pH 7-8.

DFT Calculation

To the best of our knowledge, dye–ligand–metal complex is nonfluorescent because of metal–ion–induced fluorescence quenching.[42] It is very similar to the Anslyn's probe displacement approach that metal complexes have been effectively used due to the high affinity between metal and biothiols.[51–54] To investigate the binding behavior of Compound 1 and Cu^{2+} and the red shift in the absorbance spectra ($\Delta\lambda_{abs}$ = 76 nm), DFT calculations were performed by utilizing the Gaussian 09.[55] The results were confirmed that the band gap between HOMO and LUMO of Compound 1 was found to

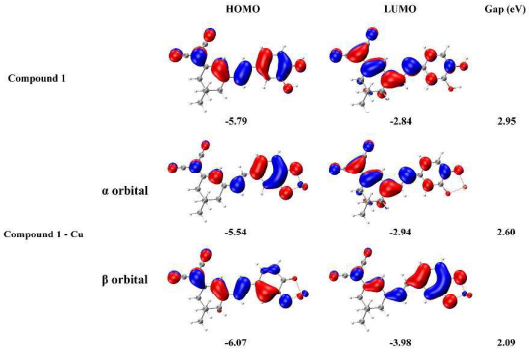

Fig. 3. Frontier molecular orbital profiles of Compound 1 and 1–Cu^{2+} based on DFT (B3LYP/cc–pVDZ) calculations.

View Article Online
DOI: 10.1039/C7TB02323E

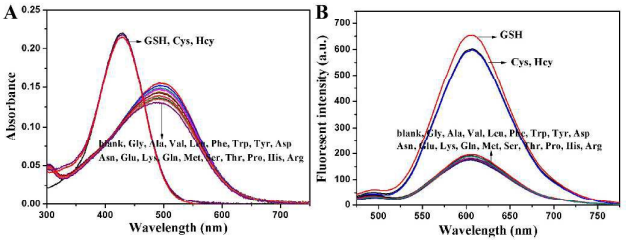

Fig. 4. UV–vis (A) and fluorescence (B) spectra of 1–Cu^{2+} in the present of GSH, Cys, Hcy (20 μM) and other amino acids (100 μM). λex = 429 nm.

be 2.95 eV. However, α orbital and β orbital of 1−Cu^{2+} ensemble were 2.60 and 2.09 eV, respectively (Fig. 3, Table S3, Table S4). These dates confirmed that there was a decrease in energy and bathochromic shift in the wavelength, which was consistent with the experimental data of absorption spectra.

Fluorescence studies of GSH with 1–Cu^{2+}

On the basis of the displacement strategy that Compound 1 could coordinated with Cu^{2+} through hydroxyl group and the subsequent complex 1–Cu^{2+} could be developed as a platform for biothiols real–time detection. To evaluate this assumption, the selectivity of 1–Cu^{2+} was examined by absorption and emission spectra (Fig. 4，Fig. S14) toward 21 kinds of amino acids (GSH, Cys, Hcy, Pro, Trp, Asp, Asn, Gly, Lys, Met, Phe, Thr, Val, Ser, Tyr, Leu, Ile, Ala, Arg, Gln, Glu). To highlight the selectivity of 1−Cu^{2+} to biothiols, the concentration of other species were ten times of the biothiols. As was shown in Fig. 4, GSH, Cys and Hcy displayed similar blue shift in absorbance spectra and fluorescence enhancement in fluorescence intensity. Additionally, there was no such spectral or visual change on fluorescence emission and absorbance spectra upon addition of other amino acids (10 equv.). Moreover, as was shown in Fig. S15, biothiols (10 μM) have a strong affinity to 1-Cu^{2+} compared to some common anion species including HS^-, $OHCH_2CH_2SH$, $(CH_3)_3SH$, PhSH (50 μM).

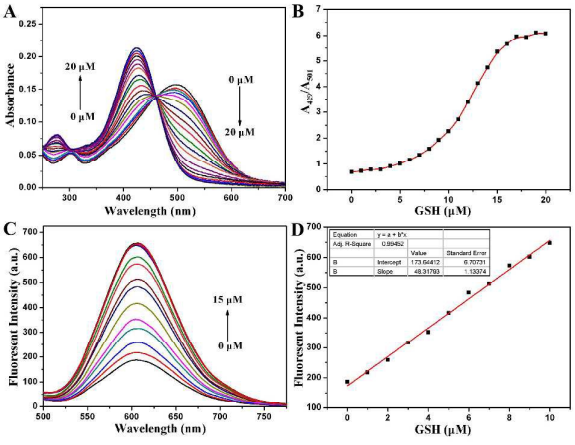

Fig. 5. (A)UV–vis of 1–Cu^{2+} (10 μM) towards different concentrations of GSH (0–20 μM) in DMSO/HEPES buffer solution (10/90, v/v, pH = 7.4, 50 mM). (B) Plots of absorbance ratio A_{429}/A_{501} vs. GSH concentration (0–20 μM). (C) Fluorescence spectra of 1–Cu^{2+} (10 μM) towards different concentrations of GSH (0–15 μM) in DMSO/HEPES buffer solution (10/90, v/v, pH = 7.4, 50 mM). and (D) Plots of fluorescence intensity ratio vs. GSH concentration (0–10 μM). λex = 429 nm

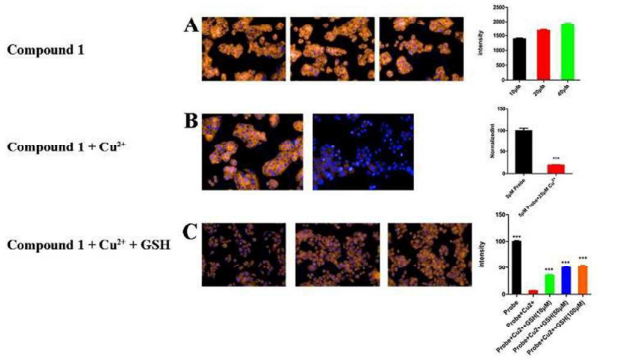

Fig. 6. (A) Fluorescence images of HepG2 cells incubated with compound 1 for 15 min (10, 20, 40 μM, respectively). (B) Fluorescence images of HepG2 cells was first incubated with Compound 1 (5 μM) for 15 min, then incubated with Cu^{2+}(25 μM) for 30 min. (C) Fluorescence images of HepG2 cells was first incubated with Compound 1 (5 μM) for 15 min, then incubated with Cu^{2+}(25 μM) for 30 min. Then, incubated with GSH (10, 50, 100 μM, respectively).

As shown in Fig. 5, 1–Cu^{2+} showed an absorption band centered around 505 nm, upon addition of GSH from 0 to 20 μM, the absorption band at 505 nm decreased, meanwhile a new band at 429 nm formed (Fig. 5 and Fig. S16), which could be detected by the naked eyes. Additionally, a distinct enhancement was observed in fluorescence spectra upon addition of GSH from 0 to 15 μM (Fig. 5C). Fig. 5D showed a good linearity (R=0.9945) toward GSH over concentration range (0−10 μM) and a detection limit of 10.3 nM. Moreover, both UV–vis and fluorescence spectra kept stable within 5 s, which was much faster than previous reports.(Table S1) Furthermore, the fluorescence responses of 1–Cu^{2+} toward biothiols were pH–dependent, and 1–Cu^{2+} could be served to detect biothiols in weakly–alkaline conditions (Fig. S17). Therefore, based on the experimental results, we could state that 1–Cu^{2+} could be employed as an OFF−ON sensor for detection of biothiols with high sensitivity and selectivity.

As shown in Fig. S18, the reversibility of Compound 1 for sequential recognition of Cu^{2+} and GSH were further investigated. Switchable changes in the emission intensity at 607 nm were observed after sequential addition of constant concentration of Cu^{2+} and GSH. This experiment could be repeated 5 times at least, implying Compound 1 could be served as a reversible OFF–ON–OFF fluorescence probe for Cu^{2+} and GSH detection.

Cell culture

To demonstrate the potential bioapplications of the probe, the ability of 1–Cu^{2+} to track GSH in living cells was determined. We firstly examined the cytotoxicity with HepG2 cells. The results showed that the viability of HepG2 cells were more than 90 % when they were incubated with 0–80 μM Compound 1 for 24 h (Fig. S19), which indicated that Compound 1 showed mildly toxicity to HepG2 cells. As shown in Fig. 6, a strong fluorescence was observed when cells incubated with Compound 1 (5 μM) for 15 min (Fig. 6A). Then, Cu^{2+}(25 μM) was added into Compound 1 treated cells, it was found that a weak fluorescence was determined in presence of Compound 1 and Cu^{2+} (25 μM) (Fig. 6B). Further, the cells were treated with GSH (10, 50, 100 μM) for 30 min, a high fluorescence was obtained again (Fig. 6C), which was due to the removal of copper from 1–Cu^{2+}. The

View Article Online
DOI: 10.1039/C7TB02323E

results demonstrated that Compound 1 and 1–Cu^{2+} can be employed to visualize Cu^{2+} and GSH in living cells, respectively.

Conclusions

In summary, we have reported a new fluorescent probe based on the displacement approach, which showed significant change in the absorbance ($\Delta\lambda_{abs}$ = 76 nm) and emission spectral behavior in the presence of copper ions in HEPES buffer. The probe showed high sensitivity toward copper ions with a low detection limit (7.34 nM), which served as an ON–OFF type probe. Complex formation of Compound 1 and Cu^{2+} was confirmed by DFT calculation and binding studies. The product of the 1–Cu^{2+} ensemble was an excellent probe for biothiols and constructed an ON−OFF−ON−type fluorescence detection system. Moreover, 1–Cu^{2+} showed a very high response speed (lower than 5s), low detection limit (10.3 nM) and a large Stokes shift (178 nm) toward biothiols. Additionally, this 1–Cu^{2+} ensemble had been applied to image GSH in living cells successfully.

Acknowledgment

The authors are grateful to financial support from Natural Science Foundation of Shanghai (No. 16ZR1408000), the National Key Program of China (No. 2016YFA0200302) and the Fundamental Research Funds for the Central Universities. And the authors would like to thank Dr Xiao-Peng He for living cells experiment.

References

[1] W. Wang, L. Li, S.F. Liu, C.P. Ma and S. Zhang, J. Am. Chem. Soc., 2008, 130, 10846–10847.
[2] D.T. Zhai, S.C. Lee, S.W. Yun and Y.T. Chang, Chem. Commun., 2013, 49, 7207–7209.
[3] W. Chen, H. Luo, X. Liu, J.W. Foley, and X. Song, Anal. Chem. , 2016, 88, 3638−3646.
[4] D. Zhang, W. Chen, J. Kang,Y. Ye, Y. Zhao and M. Xian, Org. Biomol. Chem., 2014, 12, 6837–6841.
[5] L. Niu, Q. Yang, H. Zheng, Y. Chen, L. Wu, C. Tung and Q. Yang, RSC Adv. , 2015, 5, 3959–3964.
[6] Z. Ye, C. Duan, Q. Hu, Y. Zhang, C. Qin and L. Zeng, J. Mater. Chem. B, 2017, 5, 3600–3606.
[7] W. Eranthie, C. Wang, M.S. Gabriel, R. Florian, K. Sagar, B.D.M Dillon, A.B. Daniel, M. Kerri, B. David and F.C. Benjamin, Nature., 2010, 468, 790–795.
[8] S. Sudha, B. Alex, S. Jacob, F.J. Paul, H.R. Irwin, B.D. Ralph, W.F. Peter and A.W. Philip, New. Eng. J. Med., 2002, 346, 476–483.
[9] A. Meister, J. Biol. Chem., 1988, 263, 17205–17208.
[10] F. Wang, L. Zhou, C. Zhao and W.H. Zhu, Chem. Sci., 2015, 6, 2584-2589.
[11] M. Li, Q. Zhai, W. Feng and G. Feng, Biosens. Bio., 2017, 87, 894-900.
[12] K. Liu, H. Shang, X. Kong and W. Lin, J. Mater. Chem. B, 2017, 5, 3836–3841.
[13] J. Vacek, B. Klejdus, J. Petrlová, L. Lojková and V. Kubáň, Analyst, 2006, 131, 1167–1174.
[14] Y. Zhang, J. Wang, W. Zheng, T. Chen, Q. Tong and D. Li, J. Mater. Chem. B, 2014, 2, 4159–4166.
[15] I. Takayo and R.K. Jon, Anal. Chem., 2002, 74, 1349–1354.
[16] D.L. Jia, F. Li, L.F. Sheng, Q. Ren, S. Dong, S.L. Xu, Y. Mu and Y.Q. Miao, Elec. Commun., 2011, 13, 1119–1122.
[17] B. Neil, D.E. Melanie, E.M. David and M. Michael, Chem. Commun., 2003, 1, 146–147.
[18] J. Fan, Z. Han, Y. Kang and X. Peng, Sci. Rep., 2016, 6, 19562–19570.
[19] Y. Yang, Q. Zhao and W. Feng, Chem. Rev., 2013, 113, 192-270.
[20] X. Chen, F. Wang, J. Hyun, T. Wei, J. Qiang, X. Ren, S. Injae and J. Yoon, Chem. Soc. Rev., 2016, 45, 2976–3016.
[21] H. Zhang, R. Liu, J. Liu, L. Li, P. Wang, S. Yao, Z. Xu and H. Sun, Chem. Sci., 2016, 7, 256–260.
[22] F. Yu, M. Gao and M. Li, Biomaterial, 2015, 63, 93-101.
[23] K. Wang, T. Leng, Y. Liu, C. Wang and W. Zhu, Sens. Actu. B, 2017, 248, 338-345.
[24] S. Li, D. Zhang, X. Xie, Y. Liu, Z. Xu, Y. Gao and Y. Ye, Sens. Actu. B, 2016, 224, 661–667.
[25] J. Tang, S. Ma, D. Zhang, Y. Liu, Y. Zhao and Y. Ye, Sens. Actu. B, 2016, 239, 106–115.
[26] J. Cheng, J. Song, H. Niu, J. Tang, D. Zhang, Y. Zhao and Y. Ye, New J. Chem., 2016, 40, 6384–6388.
[27] H. Jung, J. Han, T. Pradhan, S. Kim, S. Lee, T. Kim, C. Kang and J. Kim, Biomaterial, 2012, 33, 945–953.
[28] M. Wei, P. Yin, Y. Shen, L. Zhang, J.H. Deng, S.Y. Xue, H. Li, B. Guo, Y. Zhang and S. Yao, Chem. Commun., 2013, 49, 4640–4642.
[29] H. Ha, D. Yoon, S. Park and H. Kim, Tetrahedron, 2011, 67, 7759–7762.
[30] S. Lim, S. Lee, S. Park and H. Kim, Tetrahedron. Lett., 2011, 52, 3902–3904.
[31] X. Dai, Z. Wang, Z. Du, J. Cui, J. Miao and B. Zhao, Anal. Chim. Acta., 2015, 900, 103–110.
[32] X. Zhang, X. Ren, Q. Xu, K. Loh and Z. Chen, Org. Lett., 2009, 11, 1257–1260.
[33] C. Xu, H. Li and B. Yin, Biosens. Bio., 2015, 72, 275–281.
[34] M. Lee, J. Han, P. Kwon, B. Sankarprasad, J. Kim and L.Jonathan, J. Am. Chem. Soc., 2012, 134, 1316−1322
[35] M. Lee, J. Kim, J. Han, B. Sankarprasad, L.Jonathan and C. Kan, J. Am. Chem. Soc., 2012, 134, 12668–12674.
[36] J. Zhang, J. Wang, J. Liu, L. Ning, X. Zhu, B. Yu, X. Liu, X. Yao and H. Zhang, Anal. Chem., 2015, 87, 4856–4863.
[37] Z. Guo, S. Nam, S. Park J. Yoon, Chem. Sci., 2012, 3, 2760–2765.
[38] M. Wang, K. Li, J. Hou, M. Wu, Z. Huang and X. Yu, J. Org. Chem., 2012, 77, 8350–8354.
[39] W. Feng, M. Li, Y. Sun, and G. Feng, Anal. Chem., 2017, 89, 6106−6112.
[40] M. Li, W. Feng, Q. Zhai and G. Feng, Biosens. Bio., 2017, 87, 894–900.
[41] B. Liu, W. Zhu, Q. hang, W. Wu, M. Xu, Z. Ning, Y. Xie and H Tian, Chem. Commun., 2009, 13, 1766–1768.
[42] Z. Ning, Q. Zhang, W. Wu, H. Pei, B. Liu and H. Tian, J. Org. Chem., 2008, 73, 3791–3797.

View Article Online
DOI: 10.1039/C7TB02323E

[43] O. Kwon, S. Kwon, M. Jazbinsek, F. Brunner, J. Seo, C. Hunziker, A. Schneider, H. Yun, Y. Lee and P. Günter, Adv. Funct. Mater., 2008, 18, 3242−3250.
[44] O. Kwon, B. Ruiz, A. Choubey, L. Mutter, A. Schneider, M. Jazbinsek, V. Gramlich and P. Günter, Chem. Mater., 2006, 18, 4049–4054.
[45] Z. Guo, W. Zhu and H. Tian, Chem. Commun., 2012, 48, 6073-6084.
[46] R. Kendall, T. Dunning and R. Harrison, J. Chem. Phys., 1992, 96, 6796–6806.
[47] T. Lu and F. Chen, J. Comput. Ch., 2012, 33, 580–592.
[48] H. Benesi, J. Hildebrand, J. Am. Chem. Soc., 1949, 71, 2703−2707.
[49] X. Cao, W. Lin, L. He, Org. Lett., 2011, 13, 4716–4719.
[50] Y. Fu, J. Zhang, H. Wang, J. Chen, P. Zhao, G. Chen, X. He, Dyes Pigm., 2016, 133, 372–379.
[51] K. Rahul, G. Amrita, S. Ajeet, G. Prachi, M. Ashwani and J. Amilan, ACS Sens., 2016, 1, 1265−1271.
[52] L. Joyce, S. Shabbir and E. Anslyn, Chem. Soc. Rev., 2010, 39, 3621−3632.
[53] K. Sakakibara, L. Joyce, T. Mori, T. Fujisawa, S. Shabbir, J. Hill, E. Anslyn and K. Ariga, Angew. Chem. Int. Ed., 2012, 51, 9643−9646.
[54] Q. Zhao, C. Huang, F. Li, Chem. Soc. Rev., 2011, 40, 2508–2524.
[55] M. Frisch, G. Trucks and H. Schlegel, Gaussian 09, Revision A, Gaussian, Inc Wallingford CT 2009.

View Article Online
DOI: 10.1039/C7TB02323E

Graphical Abstract:

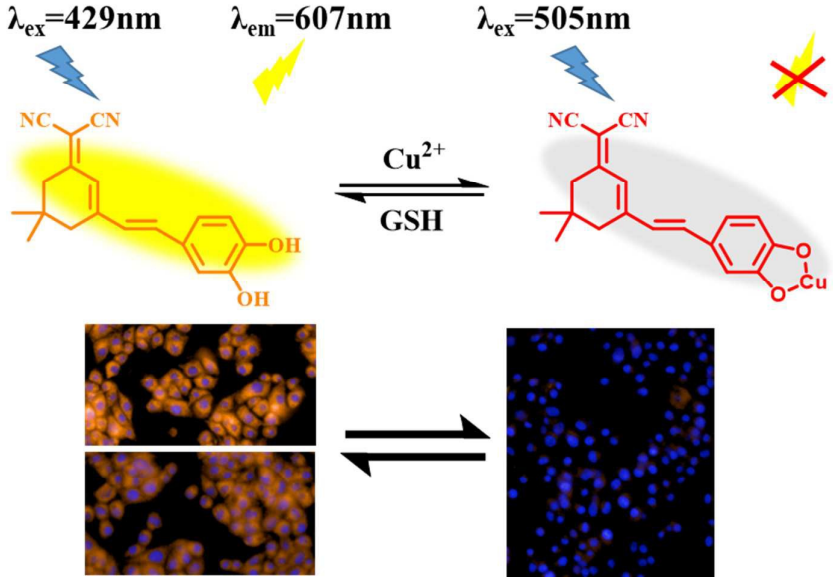

A new colorimetric and fluorescent probe with a large stokes shift for rapid and specific detection of biothiols and its application in living cells